Hadronization effects in event-shape moments

Gehrmann, T ; Jaquier, M ; Luisoni, G

Abstract: We study the moments of hadronic event shapes in e + e - annihilation within the context of next-to-next-to-leading order (NNLO) perturbative QCD predictions combined with non-perturbative power corrections in the dispersive model. This model is extended to match the NNLO perturbative prediction. The resulting theoretical expression has been compared to experimental data from JADE and OPAL, and a new value for s (M Z) has been determined, as well as of the average coupling 0 in the non-perturbative region below I =2 GeV within the dispersive model: beginarrayrcl _s(M_Z)=0.1153±0.0017(exp)±0.0023(th),

$5pt]_0 = 0.5132ś0.0115(exp)ś0.0381(th).Theprecisionofthes(MZ)valuehasbeenimprovedincomparisontothepreviouslyav$

DOI: https://doi.org/10.1140/epjc/s10052-010-1288-4

Originally published at:
Gehrmann, T; Jaquier, M; Luisoni, G (2010). Hadronization effects in event-shape moments. European Physical Journal C - Particles and Fields, 67(1-2):57-72.
DOI: https://doi.org/10.1140/epjc/s10052-010-1288-4

ZU-TH 14/09

Hadronization effects in event shape moments

T. Gehrmann, M. Jaquier and G. Luisoni

Institut für Theoretische Physik, Universität Zürich, Winterthurerstrasse 190, CH-8057 Zürich, Switzerland

Abstract

We study the moments of hadronic event shapes in e^+e^- annihilation within the context of next-to-next-to-leading order (NNLO) perturbative QCD predictions combined with non-perturbative power corrections in the dispersive model. This model is extended to match upon the NNLO perturbative prediction. The resulting theoretical expression has been compared to experimental data from JADE and OPAL, and a new value for $\alpha_s(M_Z)$ has been determined, as well as of the average coupling α_0 in the non-perturbative region below $\mu_I = 2$ GeV within the dispersive model:

$$\alpha_s(M_Z) = 0.1153 \pm 0.0017(\text{exp}) \pm 0.0023(\text{th}),$$
$$\alpha_0 = 0.5132 \pm 0.0115(\text{exp}) \pm 0.0381(\text{th}),$$

The precision of the $\alpha_s(M_Z)$ value has been improved in comparison to the previously available next-to-leading order analysis.

1 Introduction

Event shape variables measure geometrical properties of hadronic final states at high energy particle collisions. They have been studied extensively at e^+e^- collider experiments, which provided a wealth of data at a variety of centre-of-mass energies. Exploiting this large energy range, one can attempt to disentangle perturbative and non-perturbative contributions (which scale differently with increasing energy) to event shape observables.

Apart from distributions of these observables, one can also study mean values and higher moments. The nth moment of an event shape observable y is defined by

$$\langle y^n \rangle = \frac{1}{\sigma_{\mathrm{had}}} \int_0^{y_{\mathrm{max}}} y^n \frac{\mathrm{d}\sigma}{\mathrm{d}y} \mathrm{d}y \, , \tag{1}$$

where y_{max} is the kinematically allowed upper limit of the observable. Moments were measured for a variety of different event shape variables in the past. The most common observables y of three-jet type are: thrust T [1] (where moments of $y = (1 - T)$ are taken), the heavy jet mass $\rho = M_H^2/s$ [2], the C-parameter [3], the wide and total jet broadenings B_W and B_T [4], and the three-to-two-jet transition parameter in the Durham algorithm Y_3 [5]. Definitions for all observables are given in, for example, Ref. [6]. Moments with $n \geq 1$ have been measured by several experiments, most extensively by JADE [7,8] and OPAL [9], but also by DELPHI [10] and L3 [11]. A combined analysis of JADE and OPAL results has been performed in Ref. [12].

As the calculation of moments involves an integration over the full phase space, they offer a way of comparing to data which is complementary to the use of distributions, where in general cuts on certain kinematic regions are applied. Furthermore, the two extreme kinematic limits – two-jet-like events and multi-jet-like events – enter with different weights in each moment: the higher the order n of the moment, the more it becomes sensitive to the multi-jet region. Therefore it is particularly interesting to study the NNLO corrections to higher moments of event shapes, as these corrections should offer a better description of the multi-jet region due to the inclusion of additional radiation at parton level.

Moments are particularly attractive in view of studying non-perturbative hadronization corrections to event shapes. In event shape distributions, one typically corrects for hadronization effects by using generic Monte Carlo event simulation programs. A recent study, carried out in the context of a precision determination of the strong coupling constant from event shape distributions [13], revealed large discrepancies between the standard event simulation programs used at LEP [14] on one hand and more modern generators [15], which incorporate recent theoretical advances, on the other hand. In the event shape distributions, it is very difficult to disentangle hadronization corrections empirically, since they typically result in a distortion of the distribution, which can not be unfolded in a straightforward manner.

In event shape moments, one expects the hadronization corrections to be additive, such that they can be divided into a perturbative and a non-perturbative contribution,

$$\langle y^n \rangle = \langle y^n \rangle_{\mathrm{pt}} + \langle y^n \rangle_{\mathrm{np}} \, , \tag{2}$$

where the non-perturbative contribution accounts for hadronization effects. Based upon the calculation of next-to-next-to-leading order (NNLO) QCD corrections to the event shape distributions, which became available recently [6, 16–20], the perturbative contribution to event shape moments is now known to NNLO [21, 22]. The non-perturbative part is suppressed by powers of λ_p/Q^p ($p \geq 1$), where $Q \equiv \sqrt{s}$ is the centre of mass energy and λ_1 is of the order of Λ_{QCD}. The functional form of λ_p has been discussed quite extensively in the literature, but as this parameter is closely linked to non-perturbative effects, it cannot be fully derived from first principles.

In this work, we use the dispersive model derived in Ref. [23–26] to compute hadronization corrections to event shape moments. This model provides analytical predictions for the power corrections, and introduces only a single new parameter α_0, which can be interpreted as the average strong coupling

in the non-perturbative region. This model has been used extensively in combination with NLO QCD perturbative calculations to study event shape moments [9,27–29]. To combine the dispersive model with the perturbative prediction at NNLO QCD, we extended its analytical expressions to compensate for all scale-dependent terms at this order. By comparing the newly derived expressions with experimental data on event shape moments, we perform a combined determination of the perturbative strong coupling constant α_s and the non-perturbative parameter α_0. Compared to previous results at NLO, we observe that inclusion of NNLO effects results in a considerably improved consistency in the parameters determined from different shape variables, and in a substantial reduction of the error on α_s.

In Section 2, we outline the structure of perturbative and non-perturbative contributions to event shape moments. The predictions of the dispersive model to power corrections are extended to NNLO in Section 3, and used to extract α_s and α_0 from experimental data in Section 4.

2 Power corrections to event shape moments

Non-perturbative power corrections can be related to infrared renormalons in the perturbative QCD expansion for the event shape variable [23, 24, 30–35]. The analysis of infrared renormalon ambiguities suggests power corrections of the form λ_p/Q^p, but cannot make unique predictions for λ_p: it is only the sum of perturbative and non-perturbative contributions in (2) that becomes well-defined [36]. Different ways to regularise the IR renormalon singularities have been worked out in the literature [37–42].

One approach is to introduce an IR cutoff μ_I and to replace the strong coupling constant below the scale μ_I by an effective coupling such that the integral of the coupling below μ_I has a finite value [23–26]

$$\frac{1}{\mu_I}\int_0^{\mu_I} dQ\, \alpha_{\text{eff}}(Q^2) = \alpha_0(\mu_I)\,. \tag{3}$$

This dispersive model for the strong coupling leads to a shift in the distributions

$$\frac{\mathrm{d}\sigma}{\mathrm{d}y}(y) = \frac{\mathrm{d}\sigma_{\text{pt}}}{\mathrm{d}y}(y - a_y\, P)\,, \tag{4}$$

where the numerical factor a_y depends on the event shape and is listed in Table 1, while P is believed to be universal and scales with the CMS energy like μ_I/Q.

By inserting (4) into the definition of the moments, one obtains:

$$\langle y^n\rangle = \int_0^{y_{\max}} \mathrm{d}y y^n \frac{1}{\sigma_{\text{had}}}\frac{\mathrm{d}\sigma}{\mathrm{d}y}(y) \tag{5}$$

$$= \int_{-a_y P}^{y_{\max}-a_y P} \mathrm{d}y (y + a_y P)^n \frac{1}{\sigma_{\text{tot}}}\frac{\mathrm{d}\sigma_{\text{pt}}}{\mathrm{d}y}(y) \tag{6}$$

$$\approx \int_0^{y_{\max}} \mathrm{d}y (y + a_y P)^n \frac{1}{\sigma_{\text{tot}}}\frac{\mathrm{d}\sigma_{\text{pt}}}{\mathrm{d}y}(y) \tag{7}$$

discarding the integration over the kinematically forbidden values of y. This leads to the the non-

event shape observable	$1-T$	C	Y_3	M_H	B_T	B_W
a_y	2	3π	0	1	1	$\frac{1}{2}$

Table 1: The a_y coefficients of the non-perturbative event shape moment prediction

perturbative predictions for the moments of y:

$$\begin{aligned}
\langle y^1\rangle &= \langle y^1\rangle_{\rm pt} + a_y P,\\
\langle y^2\rangle &= \langle y^2\rangle_{\rm pt} + 2\langle y^1\rangle_{\rm pt}(a_y P) + (a_y P)^2,\\
\langle y^3\rangle &= \langle y^3\rangle_{\rm pt} + 3\langle y^2\rangle_{\rm pt}(a_y P) + 3\langle y^1\rangle_{\rm pt}(a_y P)^2 + (a_y P)^3,\\
\langle y^4\rangle &= \langle y^4\rangle_{\rm pt} + 4\langle y^3\rangle_{\rm pt}(a_y P) + 6\langle y^2\rangle_{\rm pt}(a_y P)^2 + 4\langle y^1\rangle_{\rm pt}(a_y P)^3 + (a_y P)^4,\\
\langle y^5\rangle &= \langle y^5\rangle_{\rm pt} + 5\langle y^4\rangle_{\rm pt}(a_y P) + 10\langle y^3\rangle_{\rm pt}(a_y P)^2 + 10\langle y^2\rangle_{\rm pt}(a_y P)^3 + 5\langle y^1\rangle_{\rm pt}(a_y P)^4 + (a_y P)^5
\end{aligned} \tag{8}$$

The perturbative contribution to $\langle y^n\rangle$ is given up to NNLO in terms of the dimensionless coefficients $\bar{\mathcal{A}}_{y,n}$, $\bar{\mathcal{B}}_{y,n}$ and $\bar{\mathcal{C}}_{y,n}$ as:

$$\begin{aligned}
\langle y^n\rangle_{\rm pt}(s,\mu^2) &= \left(\frac{\alpha_s(\mu)}{2\pi}\right)\bar{\mathcal{A}}_{y,n} + \left(\frac{\alpha_s(\mu)}{2\pi}\right)^2\left(\bar{\mathcal{B}}_{y,n} + \bar{\mathcal{A}}_{y,n}\beta_0\log\frac{\mu^2}{s}\right)\\
&\quad + \left(\frac{\alpha_s(\mu)}{2\pi}\right)^3\left(\bar{\mathcal{C}}_{y,n} + 2\bar{\mathcal{B}}_{y,n}\beta_0\log\frac{\mu^2}{s} + \bar{\mathcal{A}}_{y,n}\left(\beta_0^2\,\log^2\frac{\mu^2}{s} + \beta_1\,\log\frac{\mu^2}{s}\right)\right)\\
&\quad + \mathcal{O}(\alpha_s^4)\,.
\end{aligned} \tag{9}$$

In here, s denotes the centre-of-mass energy squared and μ is the QCD renormalisation scale. The NLO expression is obtained by suppressing all terms at order α_s^3. The first two coefficients of the QCD β-function are

$$\begin{aligned}
\beta_0 &= \frac{11C_A - 4T_R N_F}{6}\,,\\
\beta_1 &= \frac{17C_A^2 - 10C_A T_R N_F - 6C_F T_R N_F}{6}\,,
\end{aligned} \tag{10}$$

with $C_A = N$, $C_F = (N^2-1)/(2N)$, $T_R = 1/2$ for $N = 3$ colours and N_F quark flavours.

The perturbative coefficients in (9) are independent on the centre-of-mass energy. They are obtained by integrating parton-level distributions, which were calculated recently to NNLO accuracy [6, 16, 18]. These parton-level calculations are based on a numerical integration of the relevant three-parton, four-parton and five-parton matrix elements, which are combined into a parton-level event generator [17,19,20] after subtraction of infrared singular configurations using the antenna subtraction method [43]. These NNLO event shape distributions were used subsequently for improved extractions of the strong coupling constant [13, 44–47], matched on all-order resummation of logarithmically enhanced corrections [46, 48], and used for power correction studies on the thrust distribution [45].

The coefficients entering the event shape moments are computed at a renormalisation scale fixed to the centre-of-mass energy, and are therefore just dimensionless numbers for each observable and each value of n. For the first five moments of the six event shape variables considered here, they were computed up to NNLO in [21, 22].

3 Dispersive model extended to NNLO

Up to now, the dispersive model for power corrections to event shapes was used in connection with NLO calculations of the perturbative part. In this context, one obtains the following, $1/Q$-dependent power correction [25]:

$$P = \frac{4C_F}{\pi^2}\cdot\mathcal{M}\cdot\left\{\alpha_0 - \left[\alpha_s(\mu_R) + \frac{\beta_0}{\pi}\,\alpha_s^2(\mu_R)\left(\ln\frac{\mu_R}{\mu_I} + 1 + \frac{K}{2\beta_0}\right) + \mathcal{O}(\alpha_s^3)\right]\right\} \times \frac{\mu_I}{Q} \tag{11}$$

with the Milan factor $\mathcal{M} = 1.49 \pm 20\%$, which is known at two loops. Its uncertainty [49] accounts for currently unknown corrections beyond this loop order. The term in square brackets amounts to the renormalon subtraction in the power corrections, expanded to NLO.

The prediction of the dispersive model can be extended to match onto the NNLO perturbative prediction, and first steps in this direction were taken already in [45] for power corrections to the thrust distribution.

The perturbative ingredients to the dispersive model are the running of the coupling constant and the relation between the $\overline{\rm MS}$-coupling and the effective coupling, whose definition [50] absorbs universal correction terms from the cusp anomalous dimension.

In the present context, we use the evolution of the coupling constant to two loops

$$\mu^2 \frac{\mathrm{d}\alpha_s(\mu)}{\mathrm{d}\mu^2} = -\alpha_s(\mu) \left[\beta_0 \left(\frac{\alpha_s(\mu)}{2\pi} \right) + \beta_1 \left(\frac{\alpha_s(\mu)}{2\pi} \right)^2 + \mathcal{O}(\alpha_s^3) \right] . \tag{12}$$

Moreover, the relation between $\overline{\rm MS}$-coupling and effective coupling reads

$$\alpha_s^{\rm eff} = \alpha_s \left[1 + K \frac{\alpha_s}{2\pi} + L \left(\frac{\alpha_s}{2\pi} \right)^2 + \mathcal{O}(\alpha_s^3) \right] \tag{13}$$

$$K = \left(\frac{67}{18} - \frac{\pi^2}{6} \right) C_A - \frac{5}{9} N_F, \tag{14}$$

$$\begin{aligned} L = {} & C_A^2 \left(\frac{245}{24} - \frac{67}{9}\frac{\pi^2}{6} + \frac{11}{6}\zeta_3 + \frac{11}{5}\left(\frac{\pi^2}{6}\right)^2 \right) + C_F N_F \left(-\frac{55}{24} + 2\zeta_3 \right) + \\ & C_A N_F \left(-\frac{209}{108} + \frac{10}{9}\frac{\pi^2}{6} - \frac{7}{3}\zeta_3 \right) + N_F^2 \left(-\frac{1}{27} \right) . \end{aligned} \tag{15}$$

The coefficient L is obtained from the three-loop cusp anomalous dimension [51, 52], which can be extracted from the three-loop corrections to the partonic splitting functions [53] or to the quark and gluon form factors [54].

The derivation of a generic power correction starts from considering a dimensionless quantity

$$F = \int_0^Q \mathrm{d}\mu f(\mu) \tag{16}$$

with

$$f(\mu) \propto a_F \alpha_s(\mu) \frac{\mu^p}{Q^{p+1}} \tag{17}$$

assuming F to be dimensionless. The value of p determines the scaling behaviour of the power correction, with $p = 0$ for the leading power correction to event shape variables.

The dispersive model assumes that in the non-perturbative range of (16) the perturbative strong coupling $\alpha_s(\mu)$ is replaced by an effective coupling that remains finite for all μ values. One defines then the value of the integral over this region by

$$\int_0^{\mu_I} \mathrm{d}\mu \, \alpha_{s,\rm IR}(\mu) \, \frac{\mu^p}{Q^{p+1}} \equiv \frac{\mu_I^{p+1}}{Q^{p+1}(p+1)} \alpha_p(\mu_I) \tag{18}$$

introducing an infrared matching scale $\mu_I, \Lambda_{\rm QCD} \ll \mu_I \ll Q$ and α_p as a non-perturbative parameter. One has then to subtract the perturbative part of (16) in the range from 0 to μ_I from the whole integral, that is, the value of (18) with α_s replaced by $\alpha_{s,\rm IR}$.

This perturbative contribution to (16) thus acquires a dependence on the renormalisation scale μ_R used in the strong coupling constant. By requiring F to be scale-independent, one can then infer logarithmic

terms in the non-perturbative contribution to (16). Applied to the event-shape power correction P (with $p = 0$), this results in

$$P = \frac{4C_F}{\pi^2}\mathcal{M}\left\{\alpha_0 - \left[\alpha_s(\mu_R) + \frac{\beta_0}{\pi}\left(1 + \ln\left(\frac{\mu_R}{\mu_I}\right) + \frac{K}{2\beta_0}\right)\alpha_s^2(\mu_R) + \left(2\beta_1\left(1 + \ln\left(\frac{\mu_R}{\mu_I}\right) + \frac{L}{2\beta_1}\right) + 8\beta_0^2\left(1 + \ln\left(\frac{\mu_R}{\mu_I}\right) + \frac{K}{2\beta_0}\right) + 4\beta_0^2\ln\left(\frac{\mu_R}{\mu_I}\right)\left(\ln\left(\frac{\mu_R}{\mu_I}\right) + \frac{K}{\beta_0}\right)\right)\frac{\alpha_s^3(\mu_R)}{4\pi^2}\right]\right\} \times \frac{\mu_I}{Q}. \tag{19}$$

Together with (9) this gives the full expression for the event shape observable moments, including perturbative and non-perturbative contributions.

For B_T and B_W there is an additional correction to (19). At NLO, the power correction to these event shape variables is given by [26]

$$P_{\langle B_W\rangle} = P\left(\frac{\pi}{\sqrt{8C_F\hat{\alpha}_s\left(1 + \frac{K\hat{\alpha}_s}{2\pi}\right)}} + \frac{3}{4} - \frac{\beta_0}{6C_F} + \eta_0\right), \tag{20}$$

$$P_{\langle B_T\rangle} = P\left(\frac{\pi}{\sqrt{4C_F\hat{\alpha}_s\left(1 + \frac{K\hat{\alpha}_s}{2\pi}\right)}} + \frac{3}{4} - \frac{\beta_0}{3C_F} + \eta_0\right) \tag{21}$$

with $\hat{\alpha}_s(Q) = \alpha_s(e^{-\frac{3}{4}}Q)$ and $\eta_0 = -0.6137$. The full NNLO expression for these has not been calculated yet. The potentially dominant NNLO terms can however be approximated by including the effective coupling to this order, resulting in

$$P_{\langle B_W\rangle} = P\left(\frac{\pi}{\sqrt{8C_F\hat{\alpha}_s\left(1 + \frac{K\hat{\alpha}_s}{2\pi} + \frac{L\hat{\alpha}_s^2}{4\pi^2}\right)}} + \frac{3}{4} - \frac{\beta_0}{6C_F} + \eta_0\right), \tag{22}$$

$$P_{\langle B_T\rangle} = P\left(\frac{\pi}{\sqrt{4C_F\hat{\alpha}_s\left(1 + \frac{K\hat{\alpha}_s}{2\pi} + \frac{L\hat{\alpha}_s^2}{4\pi^2}\right)}} + \frac{3}{4} - \frac{\beta_0}{3C_F} + \eta_0\right). \tag{23}$$

However, further NNLO corrections to this expression will reside in the coefficient η_0. Therefore, we will treat B_W and B_T separately from the other variables in the numerical studies in the following section.

4 Analysis of JADE and OPAL data

The theoretical expressions for event shapes derived in the previous section contain two parameters: the strong coupling constant $\alpha_s(M_Z)$ and the non-perturbative coupling parameter α_0. Using experimental data on event shape moments, it is possible to fit these parameters. The data from the JADE and OPAL experiments [8] consists of 18 points at centre-of-mass energies between 14.0 and 206.6 GeV for the first

	nominal value	up variation	down variation
μ_I[GeV]	2	3	1
x_μ	1	2	0.5
$\mathcal{M}$	1.49	1.788 (+20%)	1.192 (-20%)

Table 2: Table of the μ_I, x_μ and $\mathcal{M}$ variations

five moments of T, C, Y_3, M_H, B_W and B_T, and have been taken from [28]. For each moment the NLO as well as the NNLO prediction was fitted with $\alpha_s(M_Z)$ and α_0 as fit parameters, except for the moments of Y_3, which have no power correction and thus are independent of α_0. For the heavy jet mass, we use only the even moments $\langle M_H^2 \rangle$ and $\langle M_H^4 \rangle$, since the theoretical prediction is in terms of $\rho = M_H^2/s$.

4.1 Fits

The fits were done using the program ROOT [55] and its χ^2 fit method. The errors used for the fit were the total errors, composed of the experimental statistic and systematic errors, added in quadrature. Based on these, ROOT returned errors on the fit which are displayed in Tables 4-15 in the appendix together with the fit results. For T and C the NNLO values of $\alpha_s(M_Z)$ and a_0 seem to be more stable throughout the moments, as at NNLO they increase less towards higher moments than at NLO. For Y_3 and ρ, where the values decrease at higher moments, this is not the case. These moments show $\alpha_s(M_Z)$ results which are significantly lower at NNLO than at NLO. The $\alpha_s(M_Z)$ values of B_W are much lower than the ones of the other observables, and do not change much from NLO to NNLO. For B_T the $\alpha_s(M_Z)$ values at NNLO are lower than at NLO. Both are exceptionally stable throughout the different moments. The α_0 values of all moments are higher at NNLO than at NLO.

4.2 Theoretical systematic errors

There are different parameters in the theoretical prediction which may influence the results displayed above, namely the matching scale μ_I, the renormalisation scale μ_R and the Milan factor $\mathcal{M}$. In order to estimate the resulting theoretical uncertainty on $\alpha_s(M_Z)$ and α_0, the fits were repeated, μ_I, μ_R and $\mathcal{M}$ being separately varied by a certain amount.

For this purpose the scaling factor $x_\mu = \frac{\mu_R}{Q}$ was introduced. The uncertainty on the corresponding parameter was then taken to be the difference between the nominal and the new value returned by ROOT. In order to get a total systematic error, the greater values of the up and down uncertainties were determined and quadratically added. As α_0 depends directly on μ_I no error was determined for this variation. For Y_3 there is only an error on $\alpha_s(M_Z)$ coming from the x_μ variation, since the theoretical description of this observable does not contain a contribution from the leading power correction, and is thus independent on μ_I and $\mathcal{M}$. At NLO the fit to the moment $\langle C^3 \rangle$ suffers from a numerical instability by scaling up $\mathcal{M}$ by 20%. The numbers reported in Table 6 refer to an up variation of 19%.

The NLO error on $\alpha_s(M_Z)$ agrees well with the values of [8]. At NNLO, it is reduced by more than half throughout all event shape observables except B_W, confirming a good description by the NNLO prediction. Unfortunately, this is not the case for the error on α_0. It does not change much from NLO to NNLO, even increasing a little in the first moments due to the higher x_μ uncertainty at NNLO and decreasing slightly at the higher moments, with exception, again, of B_W. Analysing the different sources of the systematical errors, we observe that the error on $\alpha_s(M_Z)$ is clearly dominated by the x_μ variation, while the largest contribution to the error on α_0 comes from the uncertainty on the Milan factor $\mathcal{M}$. Since this uncertainty has not been improved in the current study, it is understandable that the systematic error on α_0 remains unchanged. This finding clearly motivates the need for a three-loop calculation of

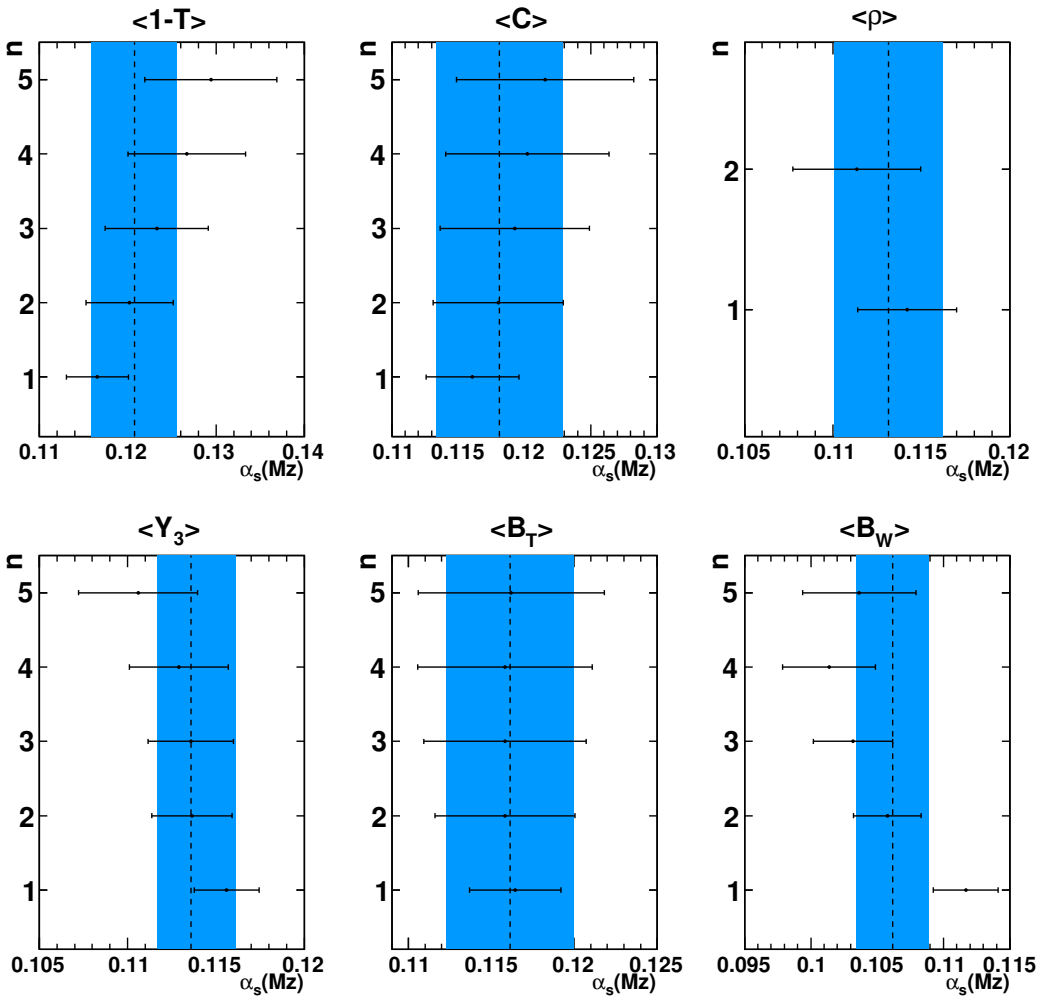

Figure 1: Plot of the individual measurements for $\alpha_s(M_Z)$. The shaded region corresponds to the error band defined by the weighted mean for the event shape and the total error on it.

the Milan factor. However, it is very important to note that the uncertainty on the Milan factor has little impact on the extraction of $\alpha_s(M_Z)$, thereby demonstrating the systematic decoupling of perturbative and non-perturbative effects in the dispersive model.

By taking the weighted means over the corresponding values from all moments of all observables one gets combined values for $\alpha_s(M_Z)$ and α_0. The weights are given by the inverse of the total error squared and are normalized such that the sum over all weights is equal to one. For the errors one has to take care of the correlation between the errors of the single measurements. The correlation matrix for $\alpha_s(M_Z)$ and α_0 is in first approximation equal to the correlation matrix for the event shape moments, since the variable transformation is linear in first approximation. The correlation matrix for the event shape moments is given in [28]. We first combine the measurements from different moments of the same observable. Figures 1 and 2 compare the combined NNLO results on the $\alpha_s(M_Z)$ and α_0 measurements. Owing to the large correlation between individual moments of the same observable, the combined errors are only marginally smaller than the errors obtained from single measurements. The combined results

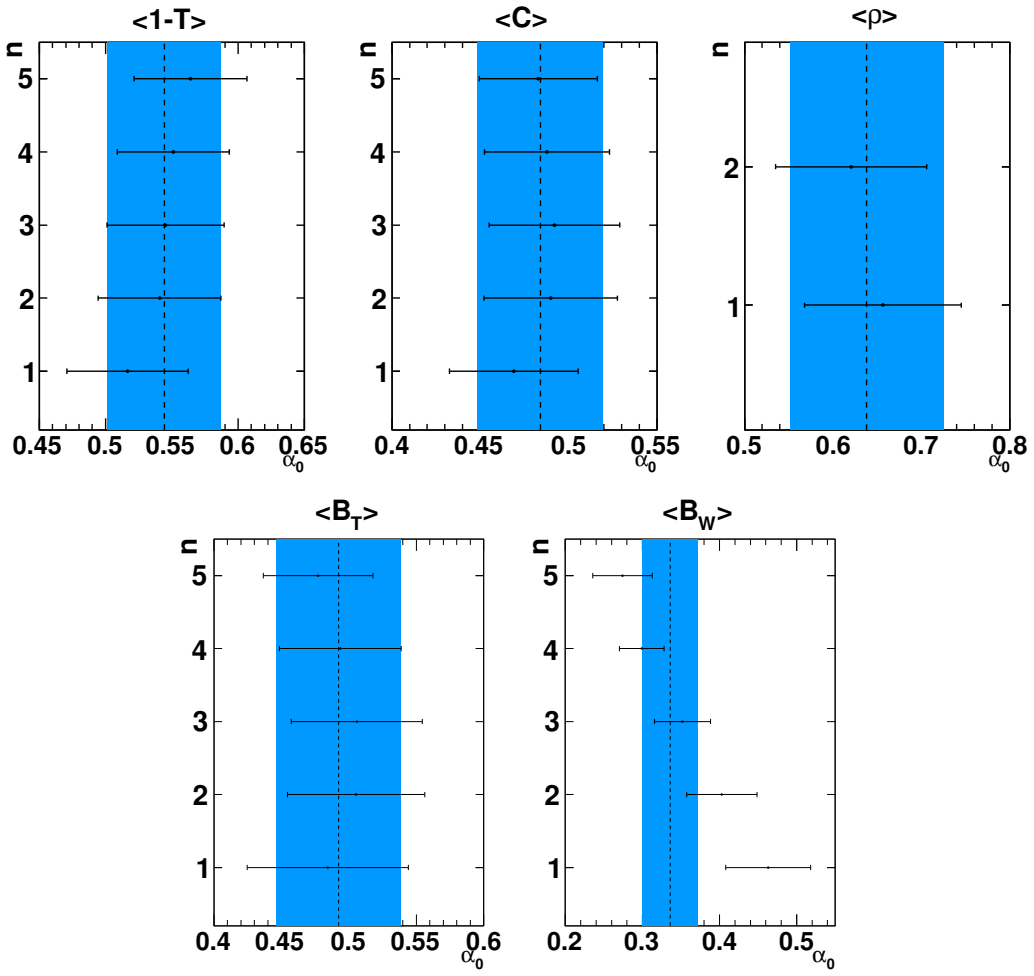

Figure 2: Error band plot of the individual measurements for α_0

and their errors are summarised in Table 3. From this Table, we clearly observe that the the theoretical error on the extraction of $\alpha_S(M_Z)$ from ρ, Y_3 and B_W is considerably smaller than from τ, C and B_T. It was observed previously in [21] that the moments of the former three shape variables receive moderate NNLO corrections for all n, while the NNLO corrections for the latter three are large already for $n = 1$ and increase with n. Consequently, the theoretical description of the moments of ρ, Y_3 and B_W displays a higher perturbative stability, which is reflected in the theoretical uncertainty on $\alpha_S(M_Z)$ derived from them.

In a second step, we combine the $\alpha_s(M_Z)$ and α_0 measurements obtained from different event shape variables. Taking the weighted mean over all values, but excluding the values for the moments of B_W and B_T where the theoretical description is incomplete, we obtain at NNLO:

$$\begin{aligned} \alpha_s(M_Z) &= 0.1153 \pm 0.0017(\text{exp}) \pm 0.0023(\text{th}), \\ \alpha_0 &= 0.5132 \pm 0.0115(\text{exp}) \pm 0.0381(\text{th})\,, \end{aligned} \tag{24}$$

where the errors have been derived taking into account the correlation between the moments of different

NNLO				
Observable	$\alpha_s(M_Z)$	Experimental Error	Theoretical Error	Total Error
τ	0.1208	0.0018	0.0045	0.0048
C	0.1181	0.0013	0.0046	0.0048
ρ	0.1131	0.0024	0.0019	0.0031
Y_3	0.1139	0.0016	0.0015	0.0022
B_T	0.1161	0.0014	0.0036	0.0038
B_W	0.1062	0.0021	0.0018	0.0027
Total	0.1131	0.0017	0.0022	0.0028
Total w/o B_T,B_W	0.1153	0.0017	0.0023	0.0028
Observable	α_0	Experimental Error	Theoretical Error	Total Error
τ	0.5444	0.0184	0.0388	0.0430
C	0.4841	0.0066	0.0347	0.0353
ρ	0.6380	0.0270	0.0824	0.0867
Y_3	-	-	-	-
B_T	0.4924	0.0102	0.0449	0.0460
B_W	0.3362	0.0125	0.0338	0.0360
Total	0.4604	0.0108	0.0359	0.0375
Total w/o B_T,B_W	0.5132	0.0115	0.0381	0.0398

Table 3: Table of the $\alpha_s(M_Z)$ and α_0 results for the individual moments and the global weighted average.

event shapes. Including the values for B_W and B_T modifies this result to:

$$\alpha_s^B(M_Z) = 0.1131 \pm 0.0017(\text{exp}) \pm 0.0022(\text{th}),$$
$$\alpha_0^B = 0.4604 \pm 0.0108(\text{exp}) \pm 0.0359(\text{th})\,.$$

These latter values are however quoted only to illustrate the impact of including the broadenings. The default fit result is (24), where only observables with a consistent theoretical description are included.

To illustrate the improvement due to the inclusion of the NNLO corrections, we also quote the corresponding NLO results. Based on τ, C, ρ and Y_3, we obtain:

$$\alpha_s^{\text{NLO}}(M_Z) = 0.1200 \pm 0.0021(\text{exp}) \pm 0.0062(\text{th}),$$
$$\alpha_0^{\text{NLO}} = 0.4957 \pm 0.0118(\text{exp}) \pm 0.0393(\text{th})\,,$$

while inclusion of B_W and B_T modifies this to

$$\alpha_s^{\text{NLO},B}(M_Z) = 0.1147 \pm 0.0020(\text{exp}) \pm 0.0046(\text{th}),$$
$$\alpha_0^{\text{NLO},B} = 0.4019 \pm 0.0130(\text{exp}) \pm 0.0296(\text{th})\,,$$

We compare the NLO and NNLO combinations in Figure 3. It can be seen very clearly that the measurements obtained from the different variables are consistent with each other within errors. The average of $\alpha_s(M_Z)$ is dominated by the measurements based on ρ and Y_3, which have the smallest theoretical uncertainties. From NLO to NNLO, the error on $\alpha_s(M_Z)$ is reduced by a factor two, and the result shifts towards the lower end of the NLO error band, as was already the case in the individual measurements. No improvement and no shift in the central value between NLO and NNLO is seen on α_0.

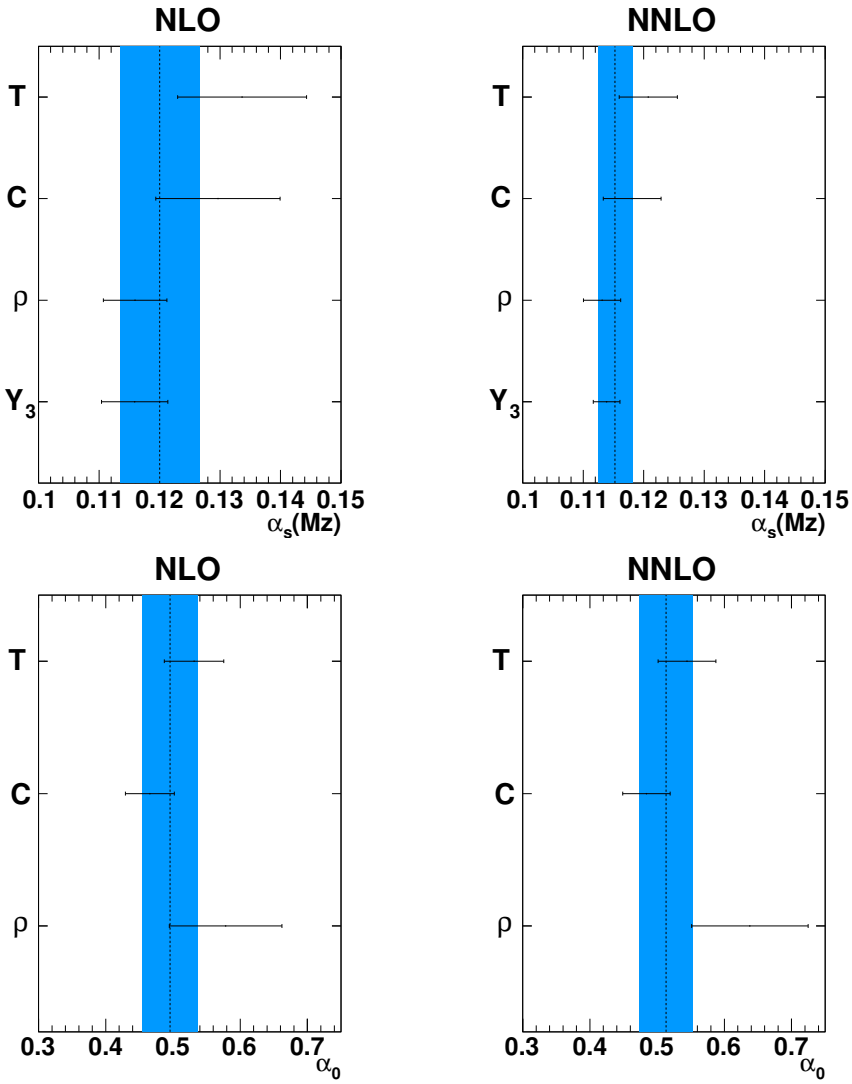

Figure 3: Error band plot of the final results. The points for $\alpha_s(M_Z)$ are C, T, Y_3, M_H and for α_0 C, T, M_H.

5 Conclusions

In this paper, we studied the perturbative and non-perturbative contributions to the moments of event shapes in e^+e^- annihilation. In view of the recently calculated NNLO perturbative contributions [21, 22] to the event shape moments, we extended the dispersive model for non-perturbative power corrections [23–25] to include all logarithmic corrections to this order. The normalisation of the power correction (the Milan factor [25]) is however still restricted to NLO accuracy, and specific corrections [26] to the jet broadenings B_W and B_T are also only included to NLO.

We used this newly obtained theoretical description of the event shape moments to reanalyse data from JADE and OPAL in view of a determination of the strong coupling constant $\alpha_s(M_Z)$ and of the non-perturbative parameter α_0. We observed that inclusion of the NNLO corrections results in a considerably

better consistency among the values extracted from different moments of the same variable, and an improved consistency among the different variables. Averaging over the different moments and different shapes (excluding B_W and B_T, where the theoretical description is incomplete, and taking proper account of the uncertainty due to missing terms in the Milan factor), we obtain the following combined values:

$$\begin{aligned} \alpha_s(M_Z) &= 0.1153 \pm 0.0017(\text{fit}) \pm 0.0023(\text{th}), \\ \alpha_0 &= 0.5132 \pm 0.0115(\text{fit}) \pm 0.0381(\text{th}) \,, \end{aligned}$$

Compared to previous NLO results, the theoretical error on $\alpha_S(M_Z)$ (which is dominated by the scale variation, improved at NNLO) is reduced by a factor of two, while the error on α_0 (which is dominated by the uncertainty on the Milan factor) remains unchanged. We observed that the sources of uncertainty on $\alpha_S(M_Z)$ and α_0 largely decouple. An improvement on α_0 will only be achievable once the three-loop corrections to the Milan factor become available.

It is noteworthy that application of the dispersive model to hadronization corrections results in a considerably lower value of $\alpha_s(M_Z)$ from event shapes than pervious studies based on Monte Carlo hadronization models [13], and in better agreement with measurements from other observables [56]. This feature has been observed previously also on the thrust distribution [45]. Revisiting the hadronization models in multi-purpose Monte Carlo programs appears to be mandatory for meaningful precision QCD studies at colliders.

Acknowledgements

We would like to thank Hasko Stenzel and Gudrun Heinrich for useful discussions. This research was supported by the Swiss National Science Foundation (SNF) under contract 200020-126691.

A Tables of results

In this appendix, we collect the extractions of $\alpha_s(M_Z)$ and α_0 at NLO and NNLO from individual moments of the six event shape variables: τ, C, ρ, Y_3, B_T, B_W.

NLO	$\langle\tau\rangle$	$\langle\tau^2\rangle$	$\langle\tau^3\rangle$	$\langle\tau^4\rangle$	$\langle\tau^5\rangle$
χ^2/dof	1.0043	1.0565	0.8399	0.6459	0.4740
$\alpha_s(M_Z)$	0.1242	0.1344	0.1416	0.1479	0.1534
Experimental Error	0.0018	0.0023	0.0028	0.0033	0.0038
x_μ variation: $x_\mu = 0.5$	-0.0054	-0.0083	-0.0101	-0.0115	-0.0129
$x_\mu = 2.0$	0.0066	0.0102	0.0123	0.0143	0.0162
μ_I variation: $\mu_I = 1.0$ Gev	0.0025	0.0035	0.0038	0.0045	0.0054
$\mu_I = 3.0$ Gev	-0.0019	-0.0025	-0.0027	-0.0031	-0.0037
$\mathcal{M}$ variation: $\mathcal{M} - 20\,\%$	0.0012	0.0016	0.0017	0.0020	0.0024
$\mathcal{M} + 20\,\%$	-0.0011	-0.0014	-0.0016	-0.0018	-0.0021
Theoretical Error	0.0072	0.0109	0.0130	0.0151	0.0172
α_0	0.4782	0.5147	0.5359	0.5521	0.5744
Experimental Error	0.0151	0.0152	0.0189	0.0222	0.0243
x_μ variation: $x_\mu = 0.5$	0.0017	0.0004	-0.0038	-0.0065	-0.0081
$x_\mu = 2.0$	-0.0000	-0.0001	0.0030	0.0051	0.0064
$\mathcal{M}$ variation: $\mathcal{M} - 20\,\%$	0.0432	0.0423	0.0405	0.0377	0.0375
$\mathcal{M} + 20\,\%$	-0.0306	-0.0307	-0.0298	-0.0284	-0.0290
Theoretical Error	0.0433	0.0423	0.0406	0.0382	0.0384

Table 4: Results for $\alpha_s(Q)$ and α_0 as obtained from fits to τ moments measured by JADE and OPAL for centre-of-mass energies between 14.0 and 206.6 GeV using theoretical NLO predictions.

NNLO	$\langle\tau\rangle$	$\langle\tau^2\rangle$	$\langle\tau^3\rangle$	$\langle\tau^4\rangle$	$\langle\tau^5\rangle$
χ^2/dof	0.9889	0.9411	0.7284	0.5526	0.3997
$\alpha_s(M_Z)$	0.1166	0.1202	0.1233	0.1267	0.1294
Experimental Error	0.0015	0.0018	0.0021	0.0024	0.0027
x_μ variation: $x_\mu = 0.5$	-0.0020	-0.0034	-0.0042	-0.0048	-0.0054
$x_\mu = 2.0$	0.0025	0.0042	0.0051	0.0058	0.0065
μ_I variation: $\mu_I = 1.0$ Gev	0.0017	0.0017	0.0017	0.0019	0.0022
$\mu_I = 3.0$ Gev	-0.0011	-0.0011	-0.0011	-0.0013	-0.0014
$\mathcal{M}$ variation: $\mathcal{M} - 20\,\%$	0.0009	0.0010	0.0009	0.0011	0.0012
$\mathcal{M} + 20\,\%$	-0.0009	-0.0009	-0.0009	-0.0010	-0.0011
Theoretical Error	0.0032	0.0046	0.0054	0.0062	0.0070
α_0	0.5165	0.5408	0.5452	0.5512	0.5641
Experimental Error	0.0135	0.0152	0.0194	0.0223	0.0246
x_μ variation: $x_\mu = 0.5$	0.0140	0.0075	0.0016	-0.0008	-0.0023
$x_\mu = 2.0$	-0.0078	-0.0045	-0.0001	0.0019	0.0031
$\mathcal{M}$ variation: $\mathcal{M} - 20\,\%$	0.0415	0.0430	0.0396	0.0357	0.0347
$\mathcal{M} + 20\,\%$	-0.0298	-0.0308	-0.0286	-0.0264	-0.0261
Theoretical Error	0.0438	0.0436	0.0397	0.0358	0.0348

Table 5: Results for $\alpha_s(Q)$ and α_0 as obtained from fits to τ moments measured by JADE and OPAL for centre-of-mass energies between 14.0 and 206.6 GeV using theoretical NNLO predictions.

NLO	$\langle C \rangle$	$\langle C^2 \rangle$	$\langle C^3 \rangle$	$\langle C^4 \rangle$	$\langle C^5 \rangle$
χ^2/dof	1.1849	1.5245	1.5651	1.5446	1.4094
$\alpha_s(M_Z)$	0.1230	0.1308	0.1347	0.1374	0.1407
Experimental Error	0.0013	0.0016	0.0020	0.0023	0.0026
x_μ variation: $x_\mu = 0.5$	-0.0052	-0.0079	-0.0091	-0.0100	-0.0108
$x_\mu = 2.0$	0.0063	0.0096	0.0111	0.0122	0.0134
μ_I variation: $\mu_I = 1.0$ Gev	0.0029	0.0045	0.0051	0.0057	0.0064
$\mu_I = 3.0$ Gev	-0.0022	-0.0031	-0.0034	-0.0038	-0.0041
$\mathcal{M}$ variation: $\mathcal{M} - 20\,\%$	0.0013	0.0020	0.0022	0.0025	0.0028
$\mathcal{M} + 20\,\%$	-0.0012	-0.0018	-0.0019	-0.0022	-0.0024
Theoretical Error	0.0071	0.0107	0.0124	0.0137	0.0151
α_0	0.4267	0.4632	0.4789	0.4839	0.4857
Experimental Error	0.0082	0.0064	0.0067	0.0069	0.0070
x_μ variation: $x_\mu = 0.5$	0.0052	0.0027	-0.0010	-0.0035	-0.0054
$x_\mu = 2.0$	-0.0029	-0.0021	0.0007	0.0027	0.0042
$\mathcal{M}$ variation: $\mathcal{M} - 20\,\%$	0.0324	0.0359	0.0377	0.0376	0.0366
$\mathcal{M} + 20\,\%$	-0.0236	-0.0266	-0.0268	-0.0283	-0.0278
Theoretical Error	0.0328	0.0360	0.0377	0.0377	0.0370

Table 6: Results for $\alpha_s(Q)$ and α_0 as obtained from fits to C moments measured by JADE and OPAL for centre-of-mass energies between 14.0 and 206.6 GeV using theoretical NLO predictions.

NNLO	$\langle C \rangle$	$\langle C^2 \rangle$	$\langle C^3 \rangle$	$\langle C^4 \rangle$	$\langle C^5 \rangle$
χ^2/dof	1.1574	1.2418	1.2353	1.1735	1.0216
$\alpha_s(M_Z)$	0.1161	0.1180	0.1193	0.1202	0.1216
Experimental Error	0.0011	0.0013	0.0016	0.0017	0.0019
x_μ variation: $x_\mu = 0.5$	-0.0020	-0.0033	-0.0039	-0.0043	-0.0046
$x_\mu = 2.0$	0.0025	0.0040	0.0047	0.0051	0.0056
μ_I variation: $\mu_I = 1.0$ Gev	0.0019	0.0022	0.0023	0.0025	0.0028
$\mu_I = 3.0$ Gev	-0.0013	-0.0014	-0.0015	-0.0016	-0.0017
$\mathcal{M}$ variation: $\mathcal{M} - 20\,\%$	0.0011	0.0012	0.0013	0.0014	0.0015
$\mathcal{M} + 20\,\%$	-0.0010	-0.0011	-0.0012	-0.0013	-0.0014
Theoretical Error	0.0033	0.0047	0.0054	0.0059	0.0064
α_0	0.4689	0.4897	0.4919	0.4877	0.4828
Experimental Error	0.0071	0.0063	0.0067	0.0069	0.0070
x_μ variation: $x_\mu = 0.5$	0.0166	0.0095	0.0053	0.0027	0.0010
$x_\mu = 2.0$	-0.0105	-0.0066	-0.0033	-0.0013	0.0001
$\mathcal{M}$ variation: $\mathcal{M} - 20\,\%$	0.0316	0.0360	0.0359	0.0346	0.0326
$\mathcal{M} + 20\,\%$	-0.0234	-0.0264	-0.0265	-0.0258	-0.0246
Theoretical Error	0.0357	0.0372	0.0363	0.0347	0.0326

Table 7: Results for $\alpha_s(Q)$ and α_0 as obtained from fits to C moments measured by JADE and OPAL for centre-of-mass energies between 14.0 and 206.6 GeV using theoretical NNLO predictions.

NLO	$\langle\rho\rangle$	$\langle\rho^2\rangle$
χ^2/dof	0.6587	0.7547
$\alpha_s(M_Z)$	0.1164	0.1152
Experimental Error	0.0023	0.0033
x_μ variation: $x_\mu = 0.5$	-0.0028	-0.0038
$x_\mu = 2.0$	0.0039	0.0049
μ_I variation: $\mu_I = 1.0$ Gev	0.0014	0.0014
$\mu_I = 3.0$ Gev	-0.0011	-0.0011
$\mathcal{M}$ variation: $\mathcal{M} - 20\,\%$	0.0006	0.0006
$\mathcal{M} + 20\,\%$	-0.0006	-0.0006
Theoretical Error	0.0042	0.0051
α_0	0.5914	0.5657
Experimental Error	0.0268	0.0361
x_μ variation: $x_\mu = 0.5$	0.0115	0.0092
$x_\mu = 2.0$	-0.0042	-0.0047
$\mathcal{M}$ variation: $\mathcal{M} - 20\,\%$	0.0795	0.0748
$\mathcal{M} + 20\,\%$	-0.0539	-0.0508
Theoretical Error	0.0803	0.0753

Table 8: Results for $\alpha_s(Q)$ and α_0 as obtained from fits to ρ moments measured by JADE and OPAL for centre-of-mass energies between 14.0 and 206.6 GeV using theoretical NLO predictions.

NNLO	$\langle\rho\rangle$	$\langle\rho^2\rangle$
χ^2/dof	0.6750	0.7607
$\alpha_s(M_Z)$	0.1142	0.1113
Experimental Error	0.0021	0.0030
x_μ variation: $x_\mu = 0.5$	-0.0009	-0.0012
$x_\mu = 2.0$	0.0013	0.0017
μ_I variation: $\mu_I = 1.0$ Gev	0.0012	0.0010
$\mu_I = 3.0$ Gev	-0.0008	-0.0007
$\mathcal{M}$ variation: $\mathcal{M} - 20\,\%$	0.0007	0.0006
$\mathcal{M} + 20\,\%$	-0.0006	-0.0006
Theoretical Error	0.0018	0.0020
α_0	0.6565	0.6208
Experimental Error	0.0224	0.0316
x_μ variation: $x_\mu = 0.5$	0.0312	0.0233
$x_\mu = 2.0$	-0.0184	-0.0143
$\mathcal{M}$ variation: $\mathcal{M} - 20\,\%$	0.0799	0.0759
$\mathcal{M} + 20\,\%$	-0.0547	-0.0518
Theoretical Error	0.0858	0.0794

Table 9: Results for $\alpha_s(Q)$ and α_0 as obtained from fits to ρ moments measured by JADE and OPAL for centre-of-mass energies between 14.0 and 206.6 GeV using theoretical NNLO predictions.

NLO	$\langle Y_3 \rangle$	$\langle Y_3^2 \rangle$	$\langle Y_3^3 \rangle$	$\langle Y_3^4 \rangle$	$\langle Y_3^5 \rangle$
χ^2/dof	0.8616	0.6386	0.7771	0.8691	0.9499
$\alpha_s(M_Z)$	0.1183	0.1172	0.1165	0.1149	0.1124
Experimental Error	0.0011	0.0016	0.0020	0.0026	0.0033
x_μ variation: $x_\mu = 0.5$	-0.0040	-0.0042	-0.0040	-0.0038	-0.0035
$x_\mu = 2.0$	0.0053	0.0054	0.0052	0.0049	0.0045
Theoretical Error	0.0047	0.0048	0.0046	0.0043	0.0040

Table 10: Results for $\alpha_s(Q)$ and α_0 as obtained from fits to Y_3 moments measured by JADE and OPAL for centre-of-mass energies between 14.0 and 206.6 GeV using theoretical NLO predictions.

NNLO	$\langle Y_3 \rangle$	$\langle Y_3^2 \rangle$	$\langle Y_3^3 \rangle$	$\langle Y_3^4 \rangle$	$\langle Y_3^5 \rangle$
χ^2/dof	0.8577	0.6581	0.7948	0.8781	0.9557
$\alpha_s(M_Z)$	0.1156	0.1136	0.1136	0.1129	0.1106
Experimental Error	0.0010	0.0015	0.0019	0.0025	0.0032
x_μ variation: $x_\mu = 0.5$	-0.0005	-0.0008	-0.0006	-0.0002	-0.0002
$x_\mu = 2.0$	0.0015	0.0017	0.0015	0.0013	0.0012
Theoretical Error	0.0010	0.0013	0.0011	0.0008	0.0007

Table 11: Results for $\alpha_s(Q)$ and α_0 as obtained from fits to Y_3 moments measured by JADE and OPAL for centre-of-mass energies between 14.0 and 206.6 GeV using theoretical NNLO predictions.

NLO	$\langle B_T \rangle$	$\langle B_T^2 \rangle$	$\langle B_T^3 \rangle$	$\langle B_T^4 \rangle$	$\langle B_T^5 \rangle$
χ^2/dof	1.5775	1.6741	1.5926	1.4005	1.1996
$\alpha_s(M_Z)$	0.1199	0.1276	0.1308	0.1327	0.1347
Experimental Error	0.0012	0.0018	0.0023	0.0027	0.0031
x_μ variation: $x_\mu = 0.5$	-0.0037	-0.0078	-0.0093	-0.0101	-0.0108
$x_\mu = 2.0$	0.0049	0.0094	0.0112	0.0123	0.0133
μ_I variation: $\mu_I = 1.0$ Gev	0.0021	0.0032	0.0036	0.0038	0.0041
$\mu_I = 3.0$ Gev	-0.0016	-0.0024	-0.0026	-0.0028	-0.0030
$\mathcal{M}$ variation: $\mathcal{M} - 20\,\%$	0.0010	0.0015	0.0016	0.0017	0.0018
$\mathcal{M} + 20\,\%$	-0.0009	-0.0014	-0.0015	-0.0016	-0.0017
Theoretical Error	0.0054	0.0101	0.0119	0.0130	0.0140
α_0	0.4252	0.4897	0.5180	0.5193	0.5088
Experimental Error	0.0130	0.0105	0.0112	0.0129	0.0146
x_μ variation: $x_\mu = 0.5$	0.0154	0.0083	0.0005	-0.0050	-0.0093
$x_\mu = 2.0$	-0.0106	-0.0074	-0.0015	0.0031	0.0070
$\mathcal{M}$ variation: $\mathcal{M} - 20\,\%$	0.0333	0.0443	0.0500	0.0493	0.0452
$\mathcal{M} + 20\,\%$	-0.0238	-0.0318	-0.0358	-0.0354	-0.0329
Theoretical Error	0.0367	0.0451	0.0501	0.0496	0.0462

Table 12: Results for $\alpha_s(Q)$ and α_0 as obtained from fits to B_T moments measured by JADE and OPAL for centre-of-mass energies between 14.0 and 206.6 GeV using theoretical NLO predictions.

NNLO	$\langle B_T \rangle$	$\langle B_T^2 \rangle$	$\langle B_T^3 \rangle$	$\langle B_T^4 \rangle$	$\langle B_T^5 \rangle$
χ^2/dof	1.6191	1.4765	1.3723	1.2059	1.0363
$\alpha_s(M_Z)$	0.1164	0.1158	0.1158	0.1158	0.1162
Experimental Error	0.0011	0.0014	0.0017	0.0019	0.0022
x_μ variation: $x_\mu = 0.5$	-0.0012	-0.0027	-0.0033	-0.0035	-0.0037
$x_\mu = 2.0$	0.0016	0.0035	0.0041	0.0044	0.0047
μ_I variation: $\mu_I = 1.0$ Gev	0.0017	0.0017	0.0018	0.0018	0.0019
$\mu_I = 3.0$ Gev	-0.0012	-0.0011	-0.0012	-0.0012	-0.0012
$\mathcal{M}$ variation: $\mathcal{M} - 20\,\%$	0.0010	0.0010	0.0010	0.0010	0.0011
$\mathcal{M} + 20\,\%$	-0.0009	-0.0009	-0.0009	-0.0009	-0.0010
Theoretical Error	0.0025	0.0040	0.0046	0.0049	0.0052
α_0	0.4844	0.5053	0.5059	0.4938	0.4772
Experimental Error	0.0104	0.0094	0.0098	0.0108	0.0117
x_μ variation: $x_\mu = 0.5$	0.0491	0.0272	0.0190	0.0142	0.0109
$x_\mu = 2.0$	-0.0295	-0.0186	-0.0129	-0.0093	-0.0066
$\mathcal{M}$ variation: $\mathcal{M} - 20\,\%$	0.0325	0.0419	0.0436	0.0415	0.0374
$\mathcal{M} + 20\,\%$	-0.0240	-0.0300	-0.0312	-0.0297	-0.0270
Theoretical Error	0.0589	0.0500	0.0476	0.0438	0.0390

Table 13: Results for $\alpha_s(Q)$ and α_0 as obtained from fits to B_T moments measured by JADE and OPAL for centre-of-mass energies between 14.0 and 206.6 GeV using theoretical NNLO predictions.

NLO	$\langle B_W \rangle$	$\langle B_W^2 \rangle$	$\langle B_W^3 \rangle$	$\langle B_W^4 \rangle$	$\langle B_W^5 \rangle$
χ^2/dof	1.5082	1.2870	1.1182	0.8965	0.6999
$\alpha_s(M_Z)$	0.1128	0.1077	0.1049	0.1023	0.1010
Experimental Error	0.0015	0.0020	0.0027	0.0033	0.0039
x_μ variation: $x_\mu = 0.5$	0.0007	-0.0028	-0.0026	-0.0022	-0.0019
$x_\mu = 2.0$	0.0006	0.0036	0.0035	0.0030	0.0027
μ_I variation: $\mu_I = 1.0$ Gev	0.0018	0.0015	0.0016	0.0016	0.0016
$\mu_I = 3.0$ Gev	-0.0014	-0.0012	-0.0012	-0.0012	-0.0013
$\mathcal{M}$ variation: $\mathcal{M} - 20\,\%$	0.0008	0.0007	0.0007	0.0007	0.0008
$\mathcal{M} + 20\,\%$	-0.0008	-0.0007	-0.0007	-0.0007	-0.0007
Theoretical Error	0.0021	0.0040	0.0039	0.0035	0.0032
α_0	0.3960	0.3552	0.3090	0.2550	0.2025
Experimental Error	0.0106	0.0132	0.0154	0.0180	0.0203
x_μ variation: $x_\mu = 0.5$	0.0870	0.0256	0.0137	0.0107	0.0089
$x_\mu = 2.0$	-0.0401	-0.0166	-0.0097	-0.0074	-0.0059
$\mathcal{M}$ variation: $\mathcal{M} - 20\,\%$	0.0357	0.0308	0.0222	0.0112	-0.0005
$\mathcal{M} + 20\,\%$	-0.0250	-0.0214	-0.0157	-0.0084	-0.0006
Theoretical Error	0.0941	0.0400	0.0261	0.0155	0.0089

Table 14: Results for $\alpha_s(Q)$ and α_0 as obtained from fits to B_W moments measured by JADE and OPAL for centre-of-mass energies between 14.0 and 206.6 GeV using theoretical NLO predictions.

NNLO	$\langle B_W \rangle$	$\langle B_W^2 \rangle$	$\langle B_W^3 \rangle$	$\langle B_W^4 \rangle$	$\langle B_W^5 \rangle$
χ^2/dof	1.5645	1.2884	1.1158	0.8943	0.7145
$\alpha_s(M_Z)$	0.1117	0.1058	0.1032	0.1014	0.1037
Experimental Error	0.0014	0.0018	0.0025	0.0031	0.0038
x_μ variation: $x_\mu = 0.5$	-0.0010	-0.0007	-0.0006	-0.0003	0.0005
$x_\mu = 2.0$	0.0007	0.0011	0.0010	0.0007	0.0001
μ_I variation: $\mu_I = 1.0$ Gev	0.0015	0.0012	0.0012	0.0012	0.0016
$\mu_I = 3.0$ Gev	-0.0010	-0.0008	-0.0008	-0.0008	-0.0011
$\mathcal{M}$ variation: $\mathcal{M} - 20\,\%$	0.0009	0.0007	0.0007	0.0007	0.0009
$\mathcal{M} + 20\,\%$	-0.0008	-0.0006	-0.0007	-0.0007	-0.0009
Theoretical Error	0.0020	0.0018	0.0017	0.0016	0.0020
α_0	0.4632	0.4029	0.3519	0.2992	0.2744
Experimental Error	0.0083	0.0110	0.0127	0.0143	0.0137
x_μ variation: $x_\mu = 0.5$	0.0393	0.0313	0.0256	0.0221	0.0358
$x_\mu = 2.0$	-0.0384	-0.0232	-0.0181	-0.0155	-0.0220
$\mathcal{M}$ variation: $\mathcal{M} - 20\,\%$	0.0378	0.0314	0.0227	0.0122	0.0045
$\mathcal{M} + 20\,\%$	-0.0270	-0.0222	-0.0163	-0.0093	-0.0045
Theoretical Error	0.0545	0.0443	0.0342	0.0252	0.0360

Table 15: Results for $\alpha_s(Q)$ and α_0 as obtained from fits to B_W moments measured by JADE and OPAL for centre-of-mass energies between 14.0 and 206.6 GeV using theoretical NNLO predictions.

References

[1] S. Brandt, C. Peyrou, R. Sosnowski and A. Wroblewski, Phys. Lett. **12** (1964) 57;
E. Farhi, Phys. Rev. Lett. **39** (1977) 1587.

[2] L. Clavelli and D. Wyler, Phys. Lett. B **103** (1981) 383.

[3] G. Parisi, Phys. Lett. B **74** (1978) 65;
J.F. Donoghue, F.E. Low and S.Y. Pi, Phys. Rev. D **20** (1979) 2759.

[4] P.E.L. Rakow and B.R. Webber, Nucl. Phys. B **191** (1981) 63;
S. Catani, G. Turnock and B. R. Webber, Phys. Lett. B **295** (1992) 269.

[5] S. Catani, Y.L. Dokshitzer, M. Olsson, G. Turnock and B.R. Webber, Phys. Lett. B **269** (1991) 432;
N. Brown and W.J. Stirling, Phys. Lett. B **252** (1990) 657; Z. Phys. C **53** (1992) 629;
W.J. Stirling *et al.*, Proceedings of the Durham Workshop, J. Phys. **G17** (1991) 1567;
S. Bethke, Z. Kunszt, D.E. Soper and W.J. Stirling, Nucl. Phys. B **370** (1992) 310 [Erratum-ibid. B **523** (1998) 681].

[6] A. Gehrmann-De Ridder, T. Gehrmann, E. W. N. Glover and G. Heinrich, JHEP **0712** (2007) 094 [arXiv:0711.4711].

[7] P. A. Movilla Fernandez, O. Biebel, S. Bethke, S. Kluth and P. Pfeifenschneider [JADE Collaboration], Eur. Phys. J. C **1** (1998) 461 [hep-ex/9708034].

[8] C. Pahl, S. Bethke, S. Kluth, J. Schieck and the JADE Collaboration, Eur. Phys. J. C **60** (2009) 181 [Erratum-ibid. C **62** (2009) 451] [arXiv:0810.2933].

[9] G. Abbiendi *et al.* [OPAL Collaboration], Eur. Phys. J. C **40** (2005) 287 [hep-ex/0503051].

[10] P. Abreu *et al.* [DELPHI Collaboration], Phys. Lett. B **456** (1999) 322.

[11] P. Achard *et al.* [L3 Collaboration], Phys. Rept. **399** (2004) 71 [hep-ex/0406049].

[12] S. Kluth, P. A. Movilla Fernandez, S. Bethke, C. Pahl and P. Pfeifenschneider, Eur. Phys. J. C **21** (2001) 199 [hep-ex/0012044].

[13] G. Dissertori, *et al.*, JHEP **0908** (2009) 036 [arXiv:0906.3436].

[14] T. Sjostrand, P. Eden, C. Friberg, L. Lonnblad, G. Miu, S. Mrenna and E. Norrbin, Comput. Phys. Commun. **135** (2001) 238 [hep-ph/0010017];
G. Corcella *et al.*, JHEP **0101** (2001) 010 [hep-ph/0011363];
L. Lonnblad, Comput. Phys. Commun. **71** (1992) 15.

[15] O. Latunde-Dada, JHEP **0711** (2007) 040 [arXiv:0708.4390];
O. Latunde-Dada, S. Gieseke and B. Webber, JHEP **0702** (2007) 051 [hep-ph/0612281].

[16] A. Gehrmann-De Ridder, T. Gehrmann, E. W. N. Glover and G. Heinrich, Phys. Rev. Lett. **99** (2007) 132002 [arXiv:0707.1285]; Phys. Rev. Lett. **100** (2008) 172001 [arXiv:0802.0813].

[17] A. Gehrmann-De Ridder, T. Gehrmann, E. W. N. Glover and G. Heinrich, JHEP **0711** (2007) 058 [arXiv:0710.0346].

[18] S. Weinzierl, JHEP **0906** (2009) 041 [arXiv:0904.1077].

[19] S. Weinzierl, JHEP **0907** (2009) 009 [arXiv:0904.1145].

[20] S. Weinzierl, Phys. Rev. Lett. **101** (2008) 162001 [arXiv:0807.3241].

[21] A. Gehrmann-De Ridder, T. Gehrmann, E. W. N. Glover and G. Heinrich, JHEP **0905** (2009) 106 [arXiv:0903.4658].

[22] S. Weinzierl, arXiv:0909.5056.

[23] Y. L. Dokshitzer, G. Marchesini and B. R. Webber, Nucl. Phys. B **469** (1996) 93 [hep-ph/9512336].

[24] Y. L. Dokshitzer and B. R. Webber, Phys. Lett. B **404** (1997) 321 [hep-ph/9704298].

[25] Y. L. Dokshitzer, A. Lucenti, G. Marchesini and G. P. Salam, JHEP **9805** (1998) 003 [hep-ph/9802381].

[26] Y. L. Dokshitzer, G. Marchesini and G. P. Salam, Eur. Phys. J. direct C **1** (1999) 3 [hep-ph/9812487].

[27] C. Pahl, S. Bethke, O. Biebel, S. Kluth and J. Schieck, arXiv:0904.0786.

[28] C. Pahl, doctoral thesis, TU Munich (2007).

[29] O. Biebel, Phys. Rept. **340** (2001) 165.

[30] A. V. Manohar and M. B. Wise, Phys. Lett. B **344** (1995) 407 [hep-ph/9406392].

[31] B. R. Webber, Phys. Lett. B **339** (1994) 148 [hep-ph/9408222].

[32] G. P. Korchemsky and G. Sterman, Nucl. Phys. B **437** (1995) 415 [hep-ph/9411211].

[33] Y. L. Dokshitzer and B. R. Webber, Phys. Lett. B **352** (1995) 451 [hep-ph/9504219].

[34] R. Akhoury and V. I. Zakharov, Phys. Lett. B **357** (1995) 646 [hep-ph/9504248].

[35] P. Nason and M. H. Seymour, Nucl. Phys. B **454** (1995) 291 [hep-ph/9506317].

[36] M. Beneke, Phys. Rept. **317** (1999) 1 [hep-ph/9807443].

[37] Y. L. Dokshitzer, A. Lucenti, G. Marchesini and G. P. Salam, Nucl. Phys. B **511** (1998) 396 [Erratum-ibid. B **593** (2001) 729] [hep-ph/9707532].

[38] G. P. Korchemsky and S. Tafat, JHEP **0010** (2000) 010 [hep-ph/0007005].

[39] A. V. Belitsky, G. P. Korchemsky and G. Sterman, Phys. Lett. B **515** (2001) 297 [hep-ph/0106308].

[40] E. Gardi and G. Grunberg, JHEP **9911** (1999) 016 [hep-ph/9908458];
E. Gardi, JHEP **0004** (2000) 030 [hep-ph/0003179];
E. Gardi and J. Rathsman, Nucl. Phys. B **609** (2001) 123 [hep-ph/0103217]; Nucl. Phys. B **638** (2002) 243 [hep-ph/0201019].

[41] J. M. Campbell, E. W. N. Glover and C. J. Maxwell, Phys. Rev. Lett. **81** (1998) 1568 [hep-ph/9803254].

[42] M. Dasgupta and G. P. Salam, J. Phys. G **30** (2004) R143 [hep-ph/0312283].

[43] A. Gehrmann-De Ridder, T. Gehrmann and E.W.N. Glover, JHEP **0509** (2005) 056 [hep-ph/0505111]; Nucl. Phys. B **691** (2004) 195 [hep-ph/0403057]; Phys. Lett. B **612** (2005) 36 [hep-ph/0501291]; **612** (2005) 49 [hep-ph/0502110].

[44] G. Dissertori, *et al.*, JHEP **0802** (2008) 040 [arXiv:0712.0327];
S. Bethke, S. Kluth, C. Pahl and J. Schieck [JADE Collaboration], arXiv:0810.1389.

[45] R.A. Davison and B.R. Webber, Eur. Phys. J. C **59** (2009) 13 [arXiv:0809.3326].

[46] T. Becher and M.D. Schwartz, JHEP **0807** (2008) 034 [arXiv:0803.0342].

[47] G. Dissertori, *et al.*, arXiv:0910.4283.

[48] T. Gehrmann, G. Luisoni and H. Stenzel, Phys. Lett. B **664** (2008) 265 [arXiv:0803.0695].

[49] Y.L. Dokshitzer, proceedings of 29th International Conference on High Energy Physics (ICHEP98), Vancouver.

[50] S. Catani, B. R. Webber and G. Marchesini, Nucl. Phys. B **349** (1991) 635.

[51] T. Becher and M. Neubert, Phys. Rev. Lett. **102** (2009) 162001 [arXiv:0901.0722]; JHEP **0906** (2009) 081 [arXiv:0903.1126].

[52] E. Gardi and L. Magnea, JHEP **0903** (2009) 079 [arXiv:0901.1091]; arXiv:0908.3273.

[53] S. Moch, J. A. M. Vermaseren and A. Vogt, Nucl. Phys. B **688** (2004) 101 [hep-ph/0403192].

[54] S. Moch, J. A. M. Vermaseren and A. Vogt, JHEP **0508** (2005) 049 [hep-ph/0507039]; Phys. Lett. B **625** (2005) 245 [hep-ph/0508055].

[55] R. Brun and F. Rademakers, Nucl. Instrum. Meth. A **389** (1997) 81.

[56] C. Amsler *et al.* [Particle Data Group], Phys. Lett. B **667** (2008) 1.